# SMILE-II: OBSERVATION OF CELESTIAL AND ATMOSPHEREIC MEV GAMMA RAYS USING A BALLOON-BORNE WIDE FIELDS OF VIEW ELECTRON-TRACKING COMPTON CAMERA

**A. Takada[1,2], T. Tanimori[1], H. Kubo[1], K. Miuchi[1], S. Kabuki[1], J. D. Parker[1], Y. Kishimoto[1], T. Mizumoto[1], K. Ueno[1], S. Kurosawa[1], S. Iwaki[1], T. Sawano[1], K. Taniue[1], K. Nakamura[1], N. Higashi[1], Y. Matsuoka[1], S. Komura[1], Y. Sato[1], S. Arvelius[3], E. Turunen[4]**

*[1]Cosmic-Ray Group, Department of Physics, Kyoto University, Email: cr-bal@cr.scphys.kyoto-u.ac.jp*
*[2]Research Institute for Sustainable Humanosphere, Kyoto University, Email: takada@rish.kyoto-u.ac.jp*
*[3]Luleå Tekniska Universitet, Email: Sachiko.Arvelius@ltu.se*
*[4]EISCAT Scientific Association, Email: esa.turunen@eiscat.se*

## ABSTRACT

We have developed an Electron Tracking Compton Camera (ETCC) as an MeV gamma-ray telescope in the next generation. The ETCC consists of a gaseous time projection chamber and a position sensitive scintillation camera. We had launched a small size ETCC loaded on a balloon in 2006, and it was successful to obtain the fluxes of diffuse cosmic and atmospheric gamma rays in the energy range between 125 keV and 1.25 MeV. As the next flight (SMILE-II), we planned a long duration flight using a circumpolar balloon launched from Kiruna, and it will observe the celestial bright sources and the atmospheric gamma-ray burst due to the relativistic electron from the radiation belt. In this paper, we report the concepts of our detector and the performance of the SMILE-II prototype.

## 1. INTRODUCTION

Observations of celestial objects in the low-energy gamma-ray band from hundreds of keV to tens of MeV provide a unique window on such phenomena as gamma-ray lines from nuclear de-excitation produced by nucleosynthesis in supernovae, electron-positron annihilation lines, and neutron capture lines from solar flares. Furthermore, radiation from black hole accretion disks has been detected, and radiation of neutral pions produced by ions accelerated in the strong gravitational potential of black holes is also expected to be detected. We can also observe synchrotron radiation or inverse Compton-scattered gamma rays in gamma-ray pulsars, active galactic nuclei (AGN), and gamma ray bursts (GRB).

However, observation of this low-energy gamma-ray is very difficult. Because the dominant process in a detector is Compton scattering and large backgrounds of photons are produced in the hadronic process between cosmic rays and a satellite body. COMPTEL, which is the first Compton camera onboard the Compton Gamma Ray Observatory, has surveyed all sky in the energy range of 0.75-30 MeV, and consisted of a position sensitive liquid scintillator, which detects the energy of recoil electron and the position of Compton scattering, and a position sensitive NaI scintillator, which detects the energy and the absorption position of scattered gamma ray. COMPTEL has rejected such background using the time of flight between two detectors, however, it discovered only approximately 30 steady gamma-ray sources [1], whereas EGRET detected 270 sources [2], and Fermi found 1451 sources during the first 11 months of the all-sky survey in the sub-GeV/GeV region above 100 MeV [3]. This reason was that the background rejection of COMPTEL was not complete and the signal to noise ratio was not so high. Therefore, for MeV astronomy, we need a new detector having wide band energy detection for the study of radiation process, a large field of view for the all sky survey, and a background rejection power for the higher detection sensitivity.

## 2. DETECTOR CONCEPTS

As a new detector satisfied these requirements, we are developing an electron-tracking Compton camera (ETCC). The schematic view is shown in Fig.1. This ETCC consists of a three-dimensional electron tracker, which detects the energy and track of recoil electron, and a position sensitive scintillator, which detects the energy and absorption point of scattered gamma ray.

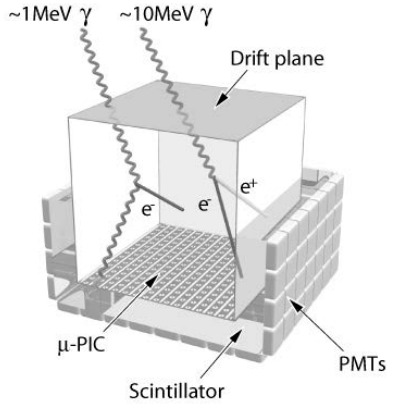


*Figure 1. Schematic view of an ETCC*

*Proc. '20th ESA Symposium on European Rocket and Balloon Programmes and Related Research'*
*Hyère, France, 22–26 May 2011 (ESA SP-700, October 2011)*

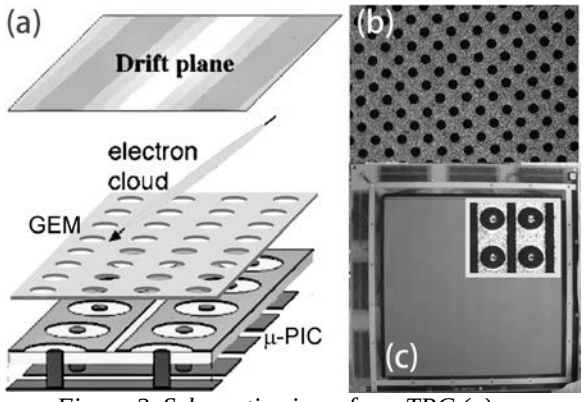


*Figure 2. Schematic view of our TPC (a), microphoto of GEM (b), photo of 30×30 cm$^2$ μ-PIC and microphoto of pixel electrode (c).*

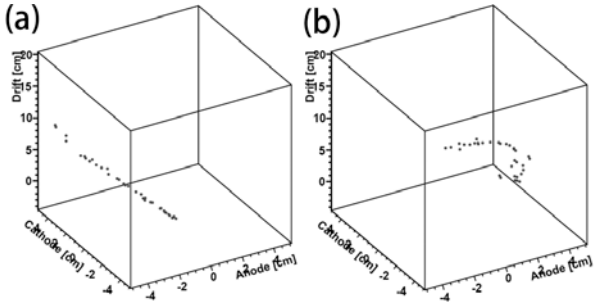


*Figure 3. Obtained tracks of cosmic muon (a) and recoil electron by gamma ray (b)*

Using the electron track, both of the energy and the direction of incident gamma ray can be reconstructed completely photon by photon. Besides, the residual angle between the scattering direction and the recoil direction provides a kinematical background rejection. This angle can be not only measured geometrically but also calculated by the kinematics of Compton scattering. Comparing these values, we can select only Compton scattering events, and obtain gamma-ray images with high signal to noise ratio.

### 2.1. Electron tracker

As the three-dimensional electron tracker, we use a time projection chamber (TPC, Fig. 2a) [4] with a micro pixel chamber: μ-PIC [5]. A μ-PIC, which is our original two-dimensional gaseous imaging detector with the micro pixel electrode made by the Print Circuit Board technology, has a fine position resolution of 120 μm (RMS) and stable high gas gain of approximately 6000 during over 1000 hour. Because it is easy to make a large area due to the PCB technology, we already developed a large μ-PIC with an area of 30×30 cm$^2$ (Fig. 2c). Using a μ-PIC with a gas electron multiplier (GEM [6], Fig. 2b), we can obtain the tracks of charged particles. When a charged particle passes through the gas, the gas around the particle track is ionized, in

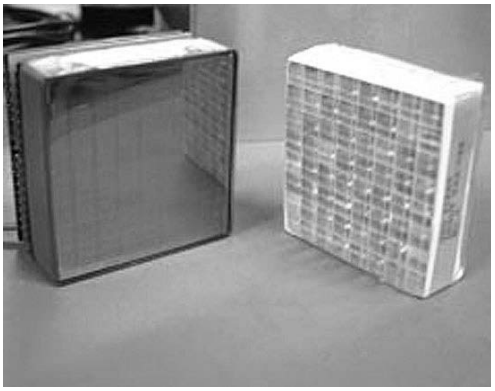

*Figure 4. Plat panel PMT (left) and GSO:Ce pixel scintillator array (right)*

which a group of ionized electron cloud are called 'electron cloud.' If there is an adequate electric field in the gas, the electron cloud drifts toward the electric field with the constant velocity. At this time, the drift time from ionized point to the termination on the anode can be transferred to the distance between the ionization point and the termination point. Therefore, if we know the start timing of the drift, the distance between the ionization point and the anode is measured by the drift time. Fig. 3 shows the tracks of charged particles obtained by 10 cm cubic TPC. Using the track of cosmic muons, we obtained the position resolution of approximately 500 μm.

### 2.2. Scattered Gamma-ray Absorber

The criteria for the scattered gamma-ray absorber are the stopping power for the gamma rays, the position resolution, and the energy resolution. Therefore, we selected the $Gd_2SiO_5$:Ce pixel scintillator arrays (PSAs) as the absorbers (right of Fig. 4) [7]. The pixel size is 6×6×13 mm$^3$, and one array consists of 8×8 pixels. For the photon sensor of the scintillator, we selected a multi-anode Flat Panel PMT H8500 made by Hamamatsu Photonics (left of Fig. 4). This PMT has 8×8 pixels with each size of 6×6 mm$^2$ and geometrical area of 52×52 mm$^2$, and its effective area is thus 89%. For the reduction of the number of readout circuit, we use the resister matrix, and obtain the position of the hit pixel using the centre of the gravity by reading 4 readouts from the corners. We make the trigger for the time projection chamber with the sum of signals from all corners. The average of energy resolution is approximately 11% at full width at half maximum (FWHM) for 662 keV.

### 2.3. SMILE project

Because the gamma ray from the celestial objects are scattered in the atmosphere, we must bring the detector over the atmosphere for the observation in the MeV

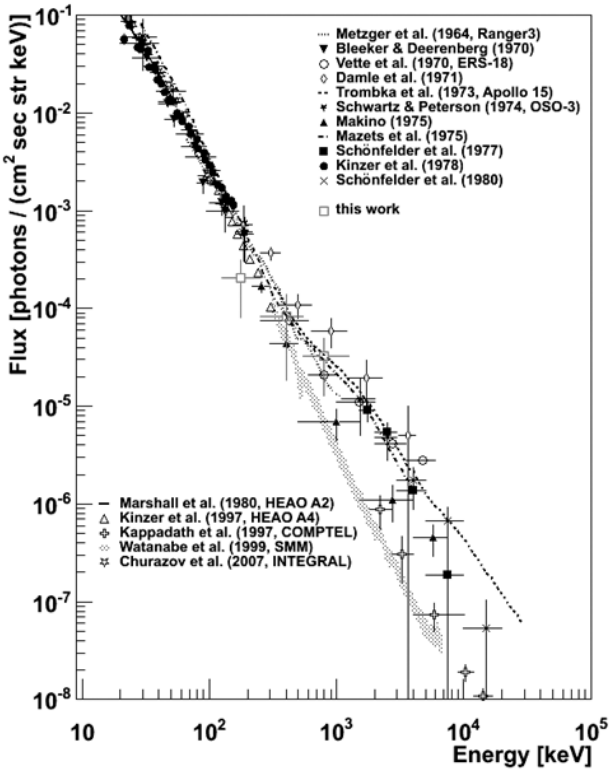


*Figure 5. Flux of the diffuse cosmic gamma rays. The opened squares represent our SMILE-I results.*

band. We have already confirmed our detector concepts by the ground base experiments [8]. Therefore, for the future observations, we have a plan of balloon experiments: "Sub-MeV gamma ray Imaging Loaded-on-balloon Experiment", called SMILE. The first step of SMILE is the operation test at the balloon altitudes and the observation of the diffuse cosmic and the atmospheric gamma rays. The second step is the observation of a bright celestial source, for example, Crab nebula, for the test of imaging properties. In future, we try to search new celestial objects in the MeV band with the long duration balloons or satellites.

As the flight model of first flight of SMILE (hereafter SMILE-I), we constructed a small size ETCC, which consisted of a 10×10×15 cm$^3$ Xe-based TPC and 33 GSO:Ce PSAs, having an effective area of approximately 1 mm$^2$ in the energy range between 150 keV and 1.5 MeV at the zenith angle less than 60 degrees [9]. The SMILE-I was launched from Sanriku Balloon Centre on September 1$^{st}$, 2006. The flight lasted during 7 hours including the level flight at the altitude of about 35 km during 4 hours (live time: 3 hours). During this flight, we obtained about 2000 reconstructed events, and 420 downward events at the level flight, which was nearly equal to the expected number of 400 events using Geant4 simulation. By the obtained growth curve, which is the dependence of the gamma-ray flux on the atmospheric depth, we calculated the fluxes of the diffuse cosmic and atmospheric gamma rays, and they were consistent with those of the other past

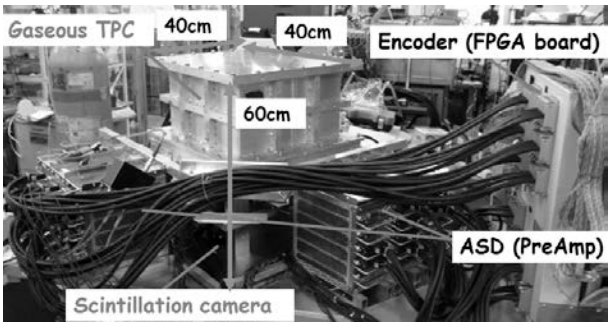


*Figure 6. Photograph of the SMILE-II prototype.*

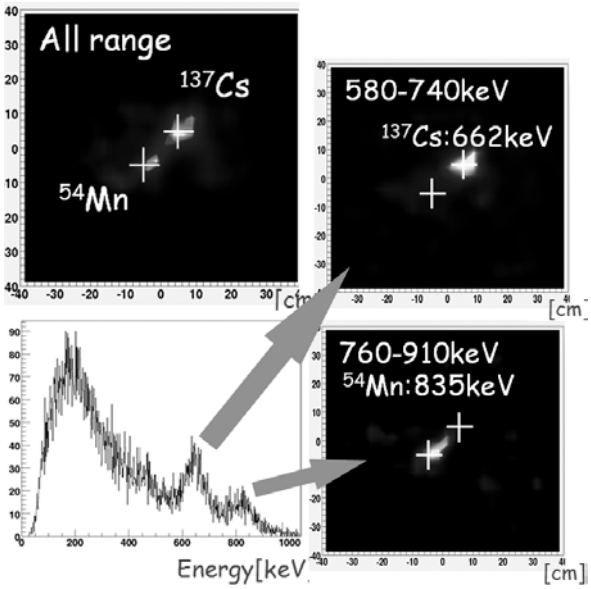


*Figure 7. Reconstructed images and energy spectrum of two different energy sources.*

observations, as shown in Fig. 5. Therefore, the ETCC of SMILE-I succeeded to observe gamma rays at the balloon altitude with rejecting other particles.

Because the SMILE-I was successful to detect gamma rays at the balloon altitude, we are preparing the next flight, SMILE-II. For the observation of a bright celestial source, we are developing an ETCC having a larger effective area using a 30 cm cubic TPC. In SMILE-II, we have two balloon flights: the first balloon is launch from Taiki Aerospace Research Field (TARF), and the purpose is the test flight for the system operation and the observation target tracking. The second is the observation of Crab nebula with a long duration flight using a circumpolar balloon launched from Kiruna. In addition, there are terrestrial gamma ray bursts due to the Relativistic Electron Precipitation (REP) on the polar region. For example, most famous burst observed at Kiruna in 1996 was detected with about 20 significances [10]. Because the ETCC loaded on SMILE-II has an angular resolution of several degrees and a large field of view of 3 sr, we can observe weak REP bursts. SMILE-II can also measure the energy spectrum and time structure of these bursts, thus we would resolve the effect of REP on the generation

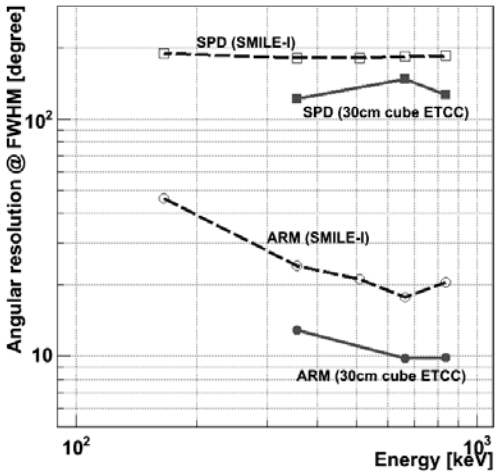


*Figure 8. Angular resolutions of SMILE-II prototype and SMILE-I flight model.*

and circulation of ozone and $NO_x$ in the upper atmosphere by the collaboration with EISCAT, which measures the radio wave from secondary or tertiary low energy electrons and ions generated by REP.

## 3. PERFORMANCE OF SMILE-II PROTOTYPE

For the purpose of SMILE-II, which is the observation of Crab nebula and the REP bursts, the criteria of the detector are an effective area larger than 0.5 $cm^2$, and an angular resolution better than 10 degrees at FWHM, for 200 keV gamma rays. Therefore, we are developing a prototype ETCC, which consists of a 30×30×30 $cm^3$ TPC and 36 GSO:Ce PSAs (Fig. 6) [11]. The energy resolutions of GSO:Ce PSAs are 11% at FWHM for 662 keV, same as that of SMILE-I. We place 6×6 PSAs at the bottom of the electron tracker. For the electron tracker of the prototype, we use a P10 gas (Ar : $C_2H_6$ = 9 : 1, in mass ratio), and we obtain a gas gain of approximately 50000. The energy resolution of this electron tracker is 50% at FWHM for 31 keV, and the position resolution of three-dimensional muon track is about 500 μm at the drift length of 15 cm.

Figure 7 shows the reconstructed images and the energy spectrum of two different energy sources obtained by the SMILE-II prototype. Each source is clearly seen in the image of the all energy range, and the energy spectrum has the peaks around source energies. When we set the energy windows at 580-740 keV and 760-910 keV, we obtained the source position of each source, as shown in Fig. 7. Therefore, the SMILE-II prototype can reconstruct both the energy and direction of the incident gamma rays correctly. Figure 8 shows the angular resolutions described by two parameters. One is the angular resolution measure (ARM), which is the accuracy of the scattering angle. The other is the scatter plane deviation (SPD), which is the decision accuracy of the scatter plane. The ARM and SPD of SMILE-II prototype are 9.8 degrees and 147 degrees at FWHM for 662 keV, respectively. Comparing with the SMILE-I

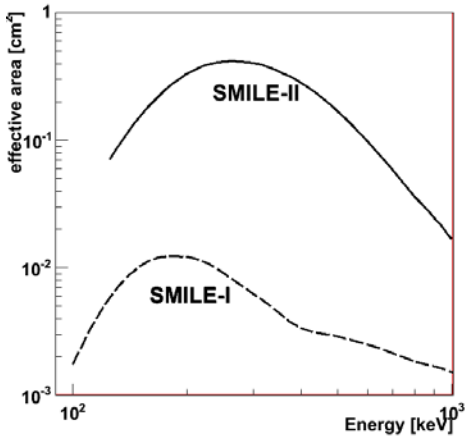


*Figure 9. Effective area of SMILE-I and SMILE-II.*

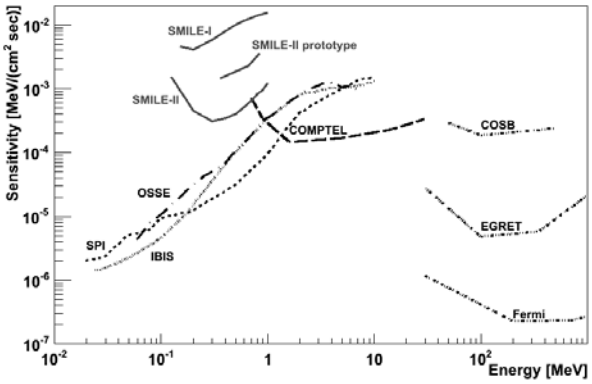


*Figure 10. Expected detection sensitivities of SMILE-I, SMILE-II prototype, and SMILE-II. ($\Delta E=E$, $T_{obs}=10^6$ sec)*

flight model, both parameter are improved. The energy resolution of the SMILE-II prototype is about 12.3% at FWHM for 662 keV, which is nearly equal to that of SMILE-I. The detection efficiency and the effective area of the SMILE-II prototype are $2.05\times10^{-5}$ and $2.05\times10^{-2}$ $cm^2$ for 662 keV.

## 4. IMPROVEMENTS FOR FLIGHT MODEL

An ETCC using a 30 cm cubic TPC is already developed, as described in Section 3, but the effective area is not enough for the SMILE-II flight model. For the purpose of SMILE-II, we need an effective area of about 0.5 $cm^2$, and the angular resolution better than 10 degrees. Hence, we are considering the improvements described as follows.

- Optimization of the TPC gas: We used a Xe based gas for the higher efficiency in SMILE-I TPC, and an Ar gas for the high gas gain in the SMILE-II prototype. The criteria of the TPC gas as a Compton target are the high electron density for the high Compton probability, the small multiple scattering and the small diffusion for the good angular resolution, the high gas gain for the stable operation. Thus we select a $CF_4$ based gas at the pressure of 1.5 atm [12].

- Expanding the absorbers: The scintillation camera covering ratio around the TPC decides the efficiency of detection of the scattered gamma rays. The flight model of SMILE-II will have 8×9 GSO:Ce PSAs at the bottom, and 36 GSO:Ce PSAs at each side of the TPC. Therefore, the geometrical area of the scintillation camera of the SMILE-II flight model will be six times larger than that of the SMILE-II prototype.
- Developing a thin and light TPC vessel: The TPC vessel placed between the effective tracking area and the scintillation camera makes the low detection efficiency, the worse energy and angular resolution, because the scattered gamma rays makes Compton scattering or absorption at the inside of the TPC vessel. Instead of the SMILE-II prototype TPC vessel, which is an aluminium vessel with the thickness of 8 mm, we are developing a thin TPC vessel.

We constructed a simulator of an ETCC including these improvements, and simulated the gamma rays detection. Figure 9 shows the effective area of SMILE-II flight model detector including these improvements and SMILE-I flight model. The effective area of SMILE-II flight model is expected to 0.5 $cm^2$ at 300 keV, which is 50 times larger than that of SMILE-I, and it is enough to observation of Crab nebula. By the result of SMILE-I, the majorities of the background events of observation using an ETCC at the balloon altitude are gamma rays, which consist of atmospheric gamma rays, diffuse cosmic gamma rays, and the instrumental gamma rays, and the effects of other particles are less than 0.2%. The ratio of the instrumental gamma rays to all background gamma rays is approximately 20%. If the intensity of the instrumental gamma rays in SMILE-II is same as that of SMILE-I, the detection sensitivity of SMILE-II is expected to be about 50 times better than the sensitivity of SMILE-I, as shown in Fig. 10.

## 5. SUMMARY

We are developing an ETCC, which consists of a three dimensional electron tracker having a fine position resolution and pixel scintillator arrays, as an MeV gamma-ray telescope in the next generation. For the future observations with a spacecraft loading, we have a plan of balloon experiments: SMILE. The first flight of SMILE was launched in 2006, and successfully obtained the fluxes of diffuse cosmic and atmospheric gamma rays at the balloon altitude. Hence, we are preparing the next flight, whose purposes are the observations of Crab nebula and REP-bursts. A SMILE-II prototype using a 30 cm cubic TPC is already developed, and we confirmed the gamma-ray detection with an ARM of 9.8 degrees and a SPD of 147 degrees at FWHM for 662 keV. In addition, we have some ideas for improving the effective area, and the SMILE-II flight model including these improvements would have approximately 50 times better detection sensitivity than that of SMILE-I. After SMILE-II, we will construct a huge ETCC by placing the 30cm cubic TPCs side by side, and we will search new MeV sources using a long duration balloon or a satellite and also observe the weak REP bursts in the polar region using a circumpolar balloon.

REFERENCES


1. Schönfelder, et al., *A&ASS*, Vol. 143, 145-179, 2000.
2. R. C. Hartman, et al., *ApJS*, Vol. 123, 79- 202, 1999.
3. A. A. Abdo, et al., *ApJS*, Vol. 188, 405-436, 2010.
4. H. Kubo, et al., *NIM A*, Vol. 513, 94-98, 2003 ; K. Miuchi, et al., *IEEE TNS*, NS-50 825-830, 2003.
5. A. Ochi, et al., *NIM A*, Vol. 471, 264-267, 2001 ; T. Nagayoshi, et al., *NIM A*, Vol. 513, 277-281, 2003.
6. F. Sauli, NIM A, Vol. 386, 531-534, 1997 ; T. Tamagawa, et al., NIM A, Vol. 560, 418-424, 2006.
7. H. Sekiya, et al., *NIM A*, Vol. 563, 49-53, 2006 ; H. Nishimura, et al., *NIM A*, Vol. 573, 115-118, 2007 ; S. Kurosawa, et al., *IEEE TNS*, Vol. 56, 3779-3788.
8. T. Tanimori, et al., *Astron. Rev.*, Vol. 48, 263-268, 2004 ; R. Orito, et al., *NIM A*, Vol. 525, 107-113, 2004 ; A. Takada, et al., *NIM A*, Vol. 546, 258-262, 2005.
9. A. Takada, et al., *ApJ*, Vol. 733, 13, 2011.
10. J. E. Foat, et al., *Geophysical Res. Lett.*, Vol. 25, 4109-4112, 1998.
11. K. Ueno, Ph. D. thesis, Kyoto University, 2011.
12. M. Takahashi, et al., *NIM A*, Vol. 628, 150-153, 2011.